

Analytic model for organic bulk heterojunction solar cells  
based on Saha equation for exciton dissociation

Sun Jiu-Xun\*, Yang Hong-Chun, Li Yang, Cui Hai-Juan

School of Physics, University of Electronic Science and Technology, Chengdu 611731, China

\* Corresponding author, E-mail: sjx@uestc.edu.cn

## Electronic Supplementary Material (ESI)

### I. Analytic solutions for drift-diffusion equations

In following paragraphs, we analytically solve current continuity equations in Eq. (2) for electrons and holes. Since we adopt the FD statistics, the boundary conditions for the carrier densities are as following forms

$$n(0) = \int_{-\infty}^{\infty} \frac{D_n(E)dE}{1 + \exp[(E_g - W_{an} + E)/kT]} \quad (S1a)$$

$$n(L) = \int_{-\infty}^{\infty} \frac{D_n(E)dE}{1 + \exp[(W_{cat} + E)/kT]} \quad (S1b)$$

$$p(0) = \int_{-\infty}^{\infty} \frac{D_p(E)dE}{1 + \exp[(W_{an} - E)/kT]} \quad (S2a)$$

$$p(L) = \int_{-\infty}^{\infty} \frac{D_p(E)dE}{1 + \exp[(E_g - W_{cat} - E)/kT]} \quad (S2b)$$

$D(E)$  is the Gaussian DOS with two parameters  $N_0$  and  $\sigma$ . For an asymmetric device,  $N_0$  and  $\sigma$  should take different values,  $N_{0n}$  and  $\sigma_n$ ,  $N_{0p}$  and  $\sigma_p$ .

$$D(E) = (N_0/\sigma\sqrt{2\pi})\exp(-E^2/2\sigma^2) \quad (S3)$$

Three auxiliary densities  $n_1$ ,  $p_1$  and  $n_i$  needed in the SRH recombination rate Eq. (11) can be expressed as follows

$$n_1 = [n(0)n(L)]^{1/2}, \quad p_1 = [p(0)p(L)]^{1/2}, \quad n_i = (n_1p_1)^{1/2} \quad (S4)$$

The degenerate coefficients  $\zeta_n$  and  $\zeta_p$  can be solved by using following method. Under the quasi-equilibrium condition, the densities of electrons and holes can be expressed as

$$n = \int_{-\infty}^{\infty} \frac{D_n(E)dE}{1 + \exp[(E - E_{Fn})/kT]} \quad (S5a)$$

$$p = \int_{-\infty}^{\infty} \frac{D_p(E)dE}{1 + \exp[(E_{Fp} - E)/kT]} \quad (S5b)$$

Introducing alternative variables  $y_n$  and  $y_p$

$$y_n = \exp(E_{Fn}/kT), \quad y_p = \exp(-E_{Fp}/kT) \quad (S6)$$

Eq. (S5) can be changed to following algebraic equations about  $y_n$  and  $y_p$

$$y_n = \frac{n}{\int_{-\infty}^{\infty} \frac{D_n(E)dE}{y_n + \exp(E/kT)}} \quad (S7a)$$

$$y_p = \frac{p}{\int_{-\infty}^{\infty} \frac{D_p(E)dE}{y_p + \exp(-E/kT)}} \quad (S7a)$$

The degenerate coefficients  $\zeta_n$  and  $\zeta_p$  can be expressed as

$$\zeta_n = \left(\frac{n}{kT}\right) \left(\frac{dn}{dE_{Fn}}\right)^{-1} = \frac{\int_{-\infty}^{\infty} \frac{D_n(E)dE}{y_n + \exp(E/kT)}}{\int_{-\infty}^{\infty} \frac{\exp(E/kT)D_n(E)dE}{[y_n + \exp(E/kT)]^2}} \quad (S8a)$$

$$\zeta_p = -\left(\frac{p}{kT}\right) \left(\frac{dp}{dE_{Fp}}\right)^{-1} = \frac{\int_{-\infty}^{\infty} \frac{D_p(E)dE}{y_p + \exp(-E/kT)}}{\int_{-\infty}^{\infty} \frac{\exp(-E/kT)D_p(E)dE}{[y_p + \exp(-E/kT)]^2}} \quad (S8a)$$

The mobility function  $\mu(F,p)$  used in this work is the improved expression of Sun et al.<sup>45</sup>

$$\mu(T,p,F) = \mu(T,p)f(T,F) \quad (S9)$$

$$\mu(T,p) = \mu_0 c_1 \exp(-c_2 \hat{\sigma}^2) \exp\left[\frac{1}{2}(\hat{\sigma}^2 - \hat{\sigma})(2p/N_0)^\delta\right] \quad (S10)$$

$$c_1 = 1.8 \times 10^{-9}, \quad c_2 = 0.5268 - 0.384aN_0^{1/3} \quad (S11)$$

$$\delta = 2\hat{\sigma}^{-2} [\ln(\hat{\sigma}^2 - \hat{\sigma}) - \ln(\ln 4)] \quad (S12)$$

$$f(T,F) = \exp\{0.44(\hat{\sigma}^{3/2} - 2.2)[\sqrt{1 + 80(eFa/\sigma)^2} - 1]\} \quad (S13)$$

Substitution of Eqs. (7, 9, 12) into Eq (5) yields,

$$C_{n2} \frac{d^2n}{dx^2} + C_{n1} \frac{dn}{dx} - (1-P)(k_n + g_n)n = -PG(x) - (1-P)R_0 \quad (S14a)$$

$$C_{p2} \frac{d^2p}{dx^2} - C_{p1} \frac{dp}{dx} - (1-P)(k_p + g_p)p = -PG(x) - (1-P)R_0 \quad (S14b)$$

with  $R_0 = R_{b0} + R_{t0}$ . Eqs. (S14) are second order linear differential equations, and can be solved as follows

$$n(x) = A_{n1}e^{\delta_{n1}x} + A_{n2}e^{\delta_{n2}x} + f_n(x) \quad (S15)$$

$$p(x) = A_{p1}e^{\delta_{p1}(L-x)} + A_{p2}e^{\delta_{p2}(L-x)} + f_p(x) \quad (S16)$$

with following characteristic roots

$$\delta_n = (2C_{n2})^{-1} \{ -C_{n1} \pm [C_{n1}^2 + 4(1-P)(k_n + g_n)C_{n2}]^{1/2} \} \quad (S17a)$$

$$\delta_p = (2C_{p2})^{-1} \{ C_{p1} \pm [C_{p1}^2 + 4(1-P)(k_p + g_p)C_{p2}]^{1/2} \} \quad (S17a)$$

and special solutions of inhomogeneous equations

$$f_n(x) = R_0/(k_n + g_n) + \int_{\lambda_1}^{\lambda_2} [B_{n1}(\lambda)e^{-\eta(\lambda)x} + B_{n2}(\lambda)e^{-\eta(\lambda)(2L-x)}] I_0(\lambda)\eta(\lambda)d\lambda \quad (S18a)$$

$$f_p(x) = R_0/(k_p + g_p) + \int_{\lambda_1}^{\lambda_2} [B_{p1}(\lambda)e^{-\eta(\lambda)x} + B_{p2}(\lambda)e^{-\eta(\lambda)(2L-x)}] I_0(\lambda)\eta(\lambda)d\lambda \quad (S18b)$$

In calculations, we follows from Kim et al.<sup>42</sup> to take  $\lambda_1 = 300$  nm,  $\lambda_2 = 1100$  nm, and normalized the incident light intensity  $P_{in}$  as 850 W/m<sup>2</sup>.

$$B_{n1} = -P[\eta^2(\lambda)C_{n2} - \eta(\lambda)C_{n1} - (1-P)(k_n + g_n)]^{-1} \quad (S19a)$$

$$B_{n2} = -P[\eta^2(\lambda)C_{n2} + \eta(\lambda)C_{n1} - (1-P)(k_n + g_n)]^{-1} \quad (S19b)$$

$$B_{p1} = -P[\eta^2(\lambda)C_{p2} + \eta(\lambda)C_{p1} - (1-P)(k_p + g_p)]^{-1} \quad (S20a)$$

$$B_{p2} = -P[\eta^2(\lambda)C_{p2} - \eta(\lambda)C_{p1} - (1-P)(k_p + g_p)]^{-1} \quad (S20b)$$

The coefficients  $A_{n1}$ ,  $A_{n2}$ ,  $A_{p1}$  and  $A_{p2}$  can be determined from the boundary conditions in Eqs.

(S1, S2), the solved expressions are as follows

$$A_{n1} = \frac{[n(0) - f_n(0)]exp(\delta_{n2}L) - n(L) + f_n(L)}{exp(\delta_{n2}L) - exp(\delta_{n1}L)} \quad (S21a)$$

$$A_{n2} = \frac{[n(0) - f_n(0)]exp(\delta_{n1}L) - n(L) + f_n(L)}{exp(\delta_{n1}L) - exp(\delta_{n2}L)} \quad (S21b)$$

$$A_{p1} = \frac{[p(L) - f_p(L)]exp(\delta_{p2}L) - p(0) + f_p(0)}{exp(\delta_{p2}L) - exp(\delta_{p1}L)} \quad (S22a)$$

$$A_{p2} = \frac{[p(L) - f_p(L)]exp(\delta_{p1}L) - p(0) + f_p(0)}{exp(\delta_{p1}L) - exp(\delta_{p2}L)} \quad (S22b)$$

## II. Additional figures

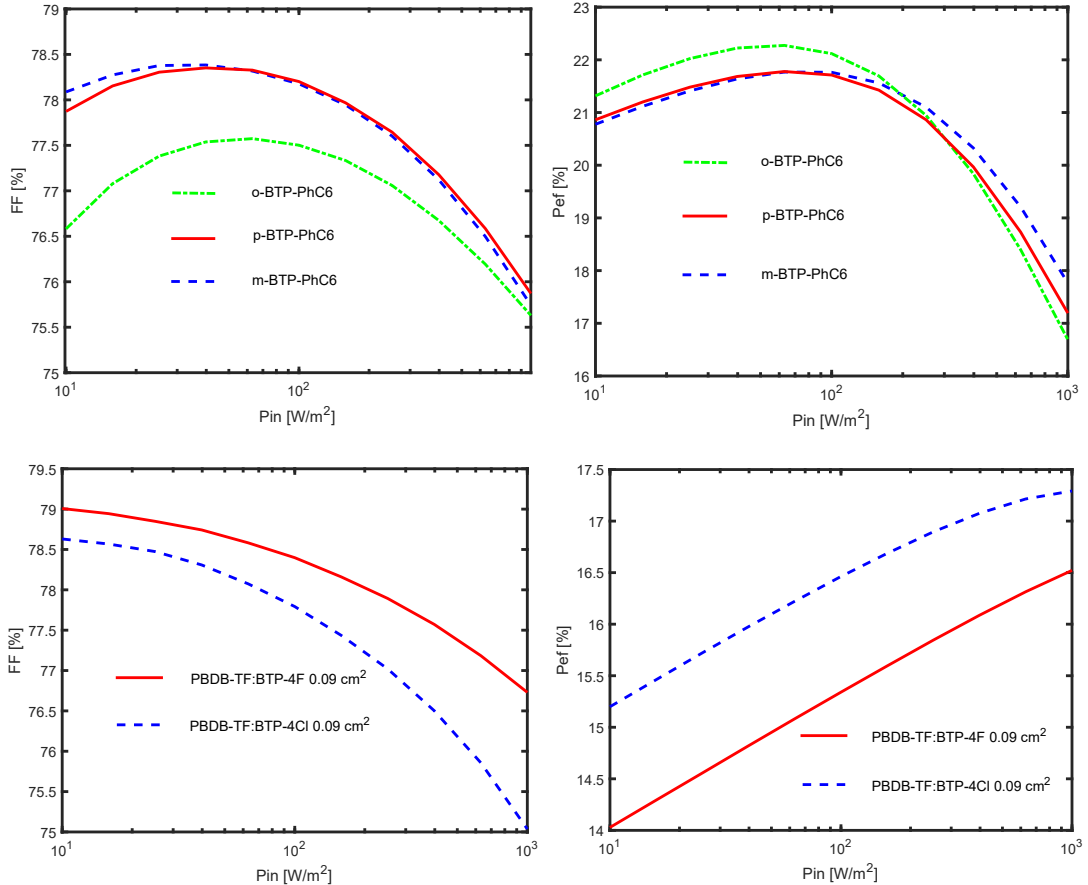


Fig. S1 Variations of  $FF$  and  $P_{ef}$  versus light intensity  $P_{in}$  for five OSCs with different materials, lines – theoretical curves with parameters in Table 1, symbols – experimental data: (a) and (b)  $FF$  -  $P_{in}$  and  $P_{ef}$  -  $P_{in}$  curves for m-BTP-PhC6, o-BTP-PhC6 and p-BTP-PhC6 materials, respectively<sup>10</sup>; (c) and (d)  $FF$  -  $P_{in}$  and  $P_{ef}$  -  $P_{in}$  curves for BTP-4Cl and BTP-4F materials, respectively<sup>6</sup>.

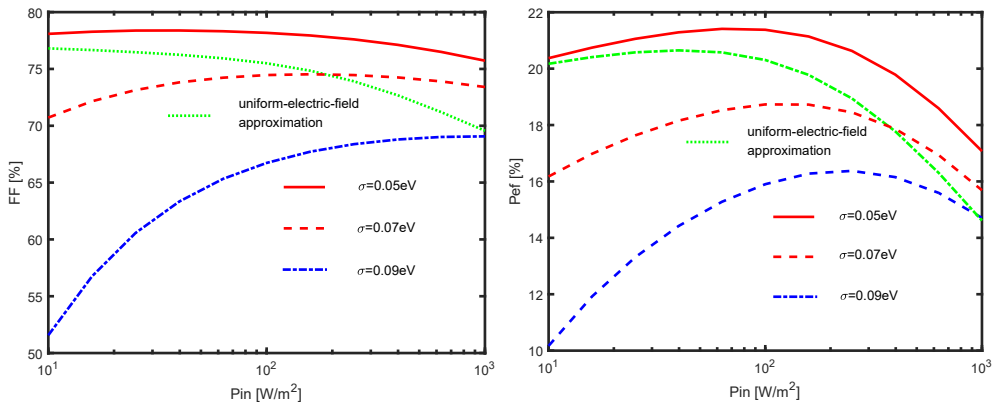


Fig. S2 Variations of  $FF$  and  $P_{ef}$  versus light intensity  $P_{in}$  for the OSC with m-BTP-PhC6 material, lines – theoretical curves with other parameters in Table 1 and  $\sigma = 0.05, 0.07, 0.09$  eV, dot line – theoretical curve with  $\sigma = 0.05$  eV and not considering SCLC effect (UEFA), respectively. (a)  $FF$  -  $P_{in}$  curves, (b)  $P_{ef}$  -  $P_{in}$  curves.

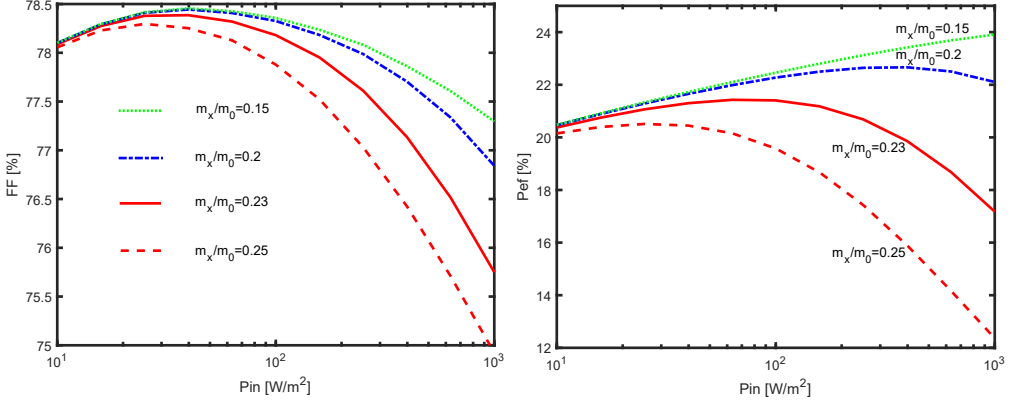


Fig. S3 Variations of  $FF$  and  $P_{ef}$  versus light intensity  $P_{in}$  for the OSC with m-BTP-PhC6 material, lines – theoretical curves with other parameters in Table 1 and  $m_x / m_0 = 0.15, 0.2, 0.23, 0.25$ , respectively. (a)  $FF$  -  $P_{in}$  curves, (b)  $P_{ef}$  -  $P_{in}$  curves.

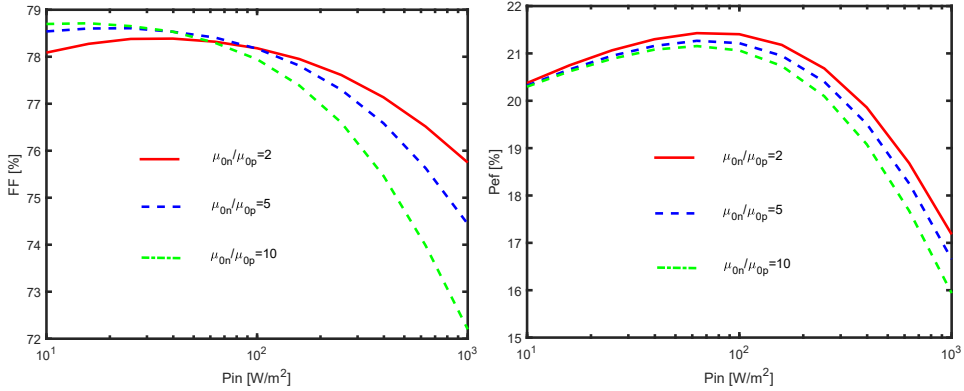


Fig. S4 Variations of  $FF$  and  $P_{ef}$  versus light intensity  $P_{in}$  for the OSC with m-BTP-PhC6 material, lines – theoretical curves with other parameters in Table 1 and with fixed  $(\mu_{0n} + \mu_{0p})$  and ratio  $\mu_{0n}/\mu_{0p} = 2, 5, 10$ , respectively. (a)  $FF$  -  $P_{in}$  curves, (b)  $P_{ef}$  -  $P_{in}$  curves.

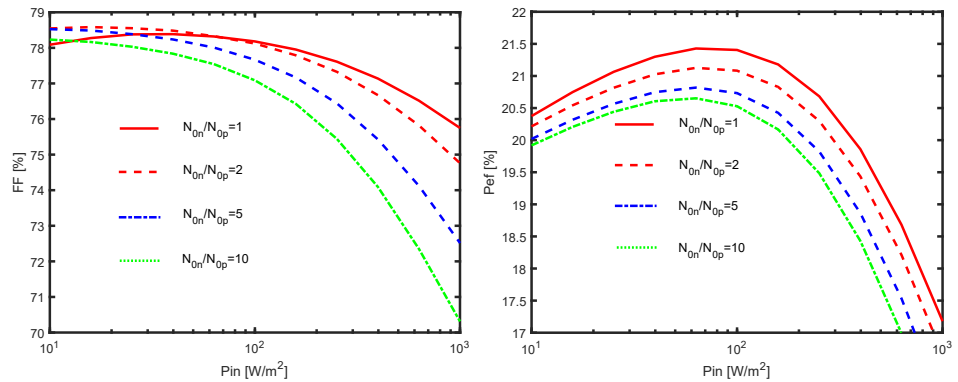


Fig. S5 Variations of  $FF$  and  $P_{ef}$  versus light intensity  $P_{in}$  for the OSC with m-BTP-PhC6 material, lines – theoretical curves with other parameters in Table 1 and with fixed  $(N_{0n} + N_{0p})$  and ratio  $N_{0n}/N_{0p} = 1, 2, 5, 10$ , respectively. (a)  $FF$  -  $P_{in}$  curves, (b)  $P_{ef}$  -  $P_{in}$  curves.

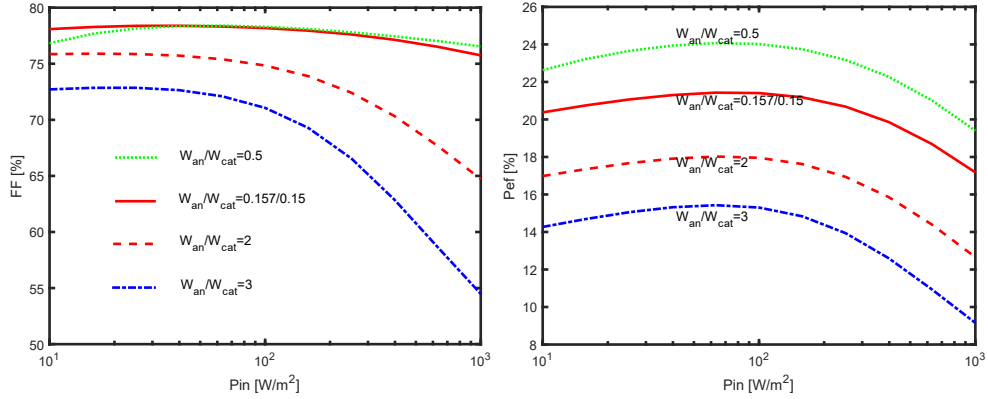


Fig. S6 Variations of  $FF$  and  $P_{ef}$  versus light intensity  $P_{in}$  for the OSC with m-BTP-PhC6 material, lines – theoretical curves with other parameters in Table 1 and with fixed ( $W_{an}+W_{cat}$ ) and ratio  $W_{an}/W_{cat} = 0.5, 0.157/0.15, 2, 3$ , respectively. (a)  $FF$  -  $P_{in}$  curves, (b)  $P_{ef}$  -  $P_{in}$  curves.

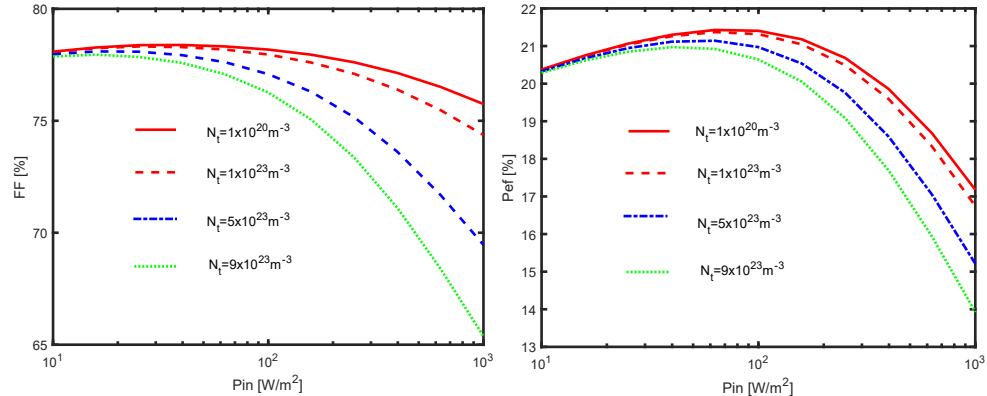
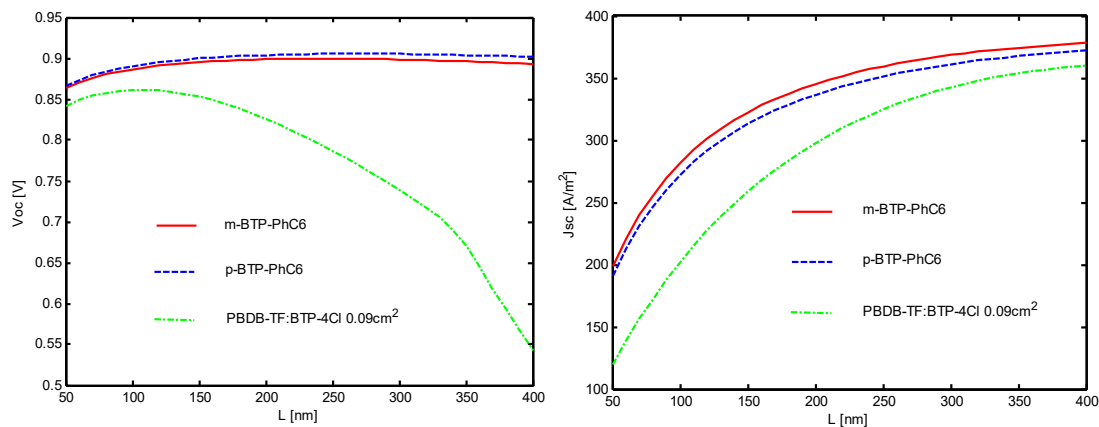


Fig. S7 Variations of  $FF$  and  $P_{ef}$  versus light intensity  $P_{in}$  for the OSC with m-BTP-PhC6 material, lines – theoretical curves with other parameters in Table 1 and with  $N_t = 1 \times 10^{20}, 1 \times 10^{23}, 5 \times 10^{23}, 9 \times 10^{23} \text{ m}^{-3}$ , respectively. (a)  $FF$  -  $P_{in}$  curves, (b)  $P_{ef}$  -  $P_{in}$  curves.



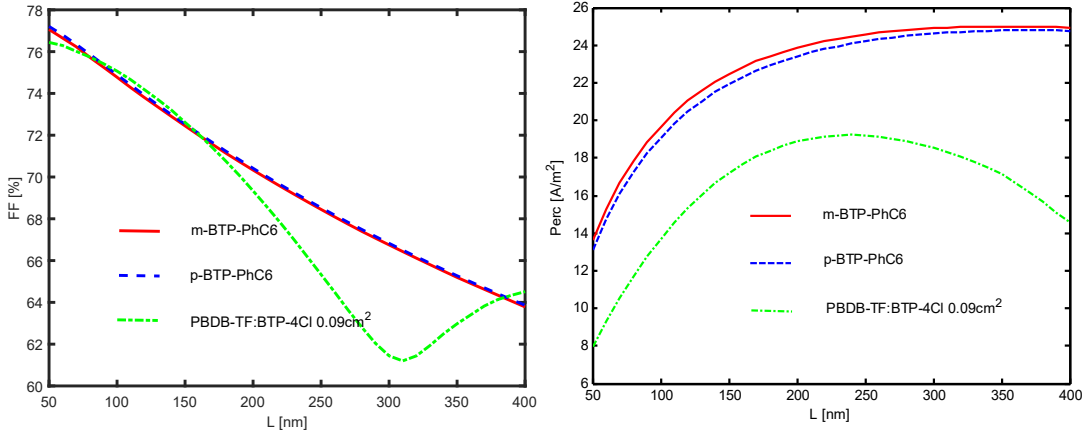
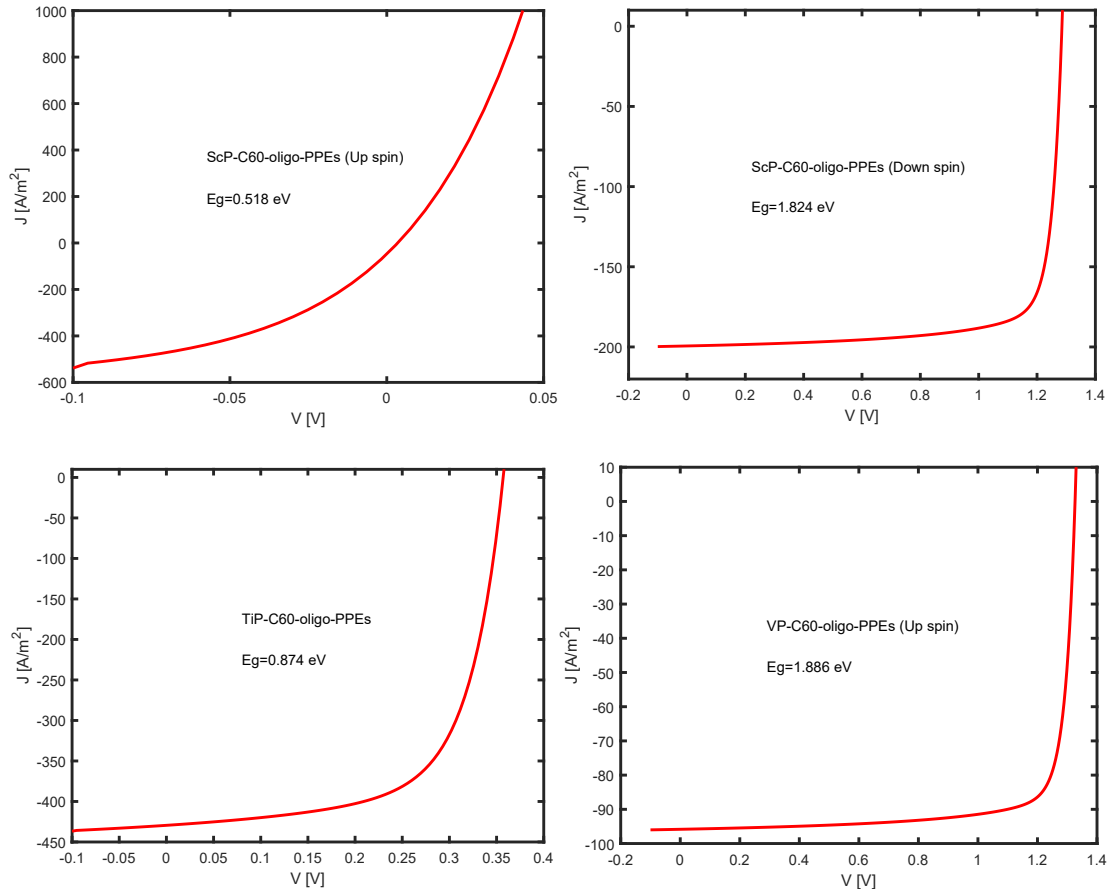
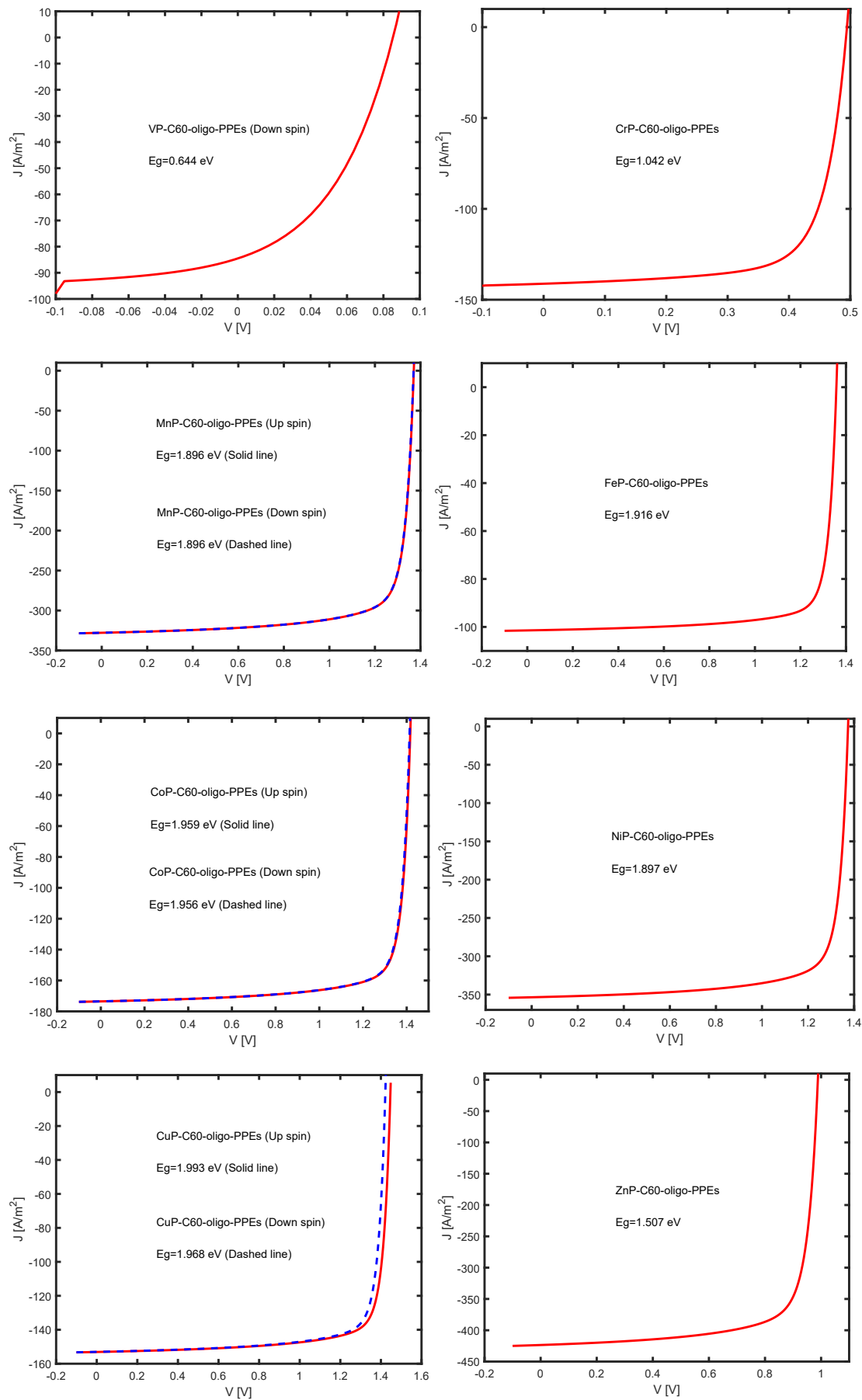


Fig. S8 Variations of performance parameters versus thickness  $L$  of active layer for three OSCs with m-BTP-PhC6, p-BTP-PhC6, and PBDB-TF: BTP-4Cl materials, lines – theoretical curves with parameters in Table 1, respectively. (a)  $V_{oc}$  -  $L$  curves, (b)  $J_{sc}$  -  $L$  curves, (c)  $FF$  -  $L$  curves, (d)  $P_{ef}$  -  $L$  curves.

### III. Predicted J-V curves for 15 compounds listed in Table 2





#### IV. MATLAB codes for calculations of J-V curves

```

351 364 348 323 295 269 250 270 298 322 350 376 408 435 465 498 529 554 562 551
527 506 479 456 436 417 400 373 343 326 335 355 376 403 ...
430 465 494 518 547 580 614 649 678 704 740 766 799 827 858 882 901 915 923 933
939 944 947 959 963 967 970 973]; % Data points from REF
xs=350+(1050-350)*(xpic-283)/(1510-283); % [nm]
yr=0+(1-0)*(ypic-973)/(250-973); % Normalized absorption (%) for 350-
1050 nm
ys=2.0E7*yr; % [to 1/m]
% Data for absorption spectrum end

AM1dot5 = xlsread('AM0AM1_5.xls'); % read data of solar spectrum
wl = (AM1dot5(43:941,1)); % [nm]
cas = interp1(xs,ys,wl,'linear'); % [1/m] Absorption spectrum
Ipa = (AM1dot5(43:243,3)); % [W/m^2/nm] Incident-light power
density
Ipб = (AM1dot5(244:941,3)); % [W/m^2/nm] Incident-light power
density
Ipд = [0.5*Ipa Ipб];
Ipф = Ipд.*((wl*1.0E-9/h/cc)); % [1/m^2/s] Incident photon flux, Step
of wave-length is 0.5 nm
Ipt0 = sum(Ipd) % [W/m^2] Total Incident-light
power density

% Defining the Material Constants %
CN = sqrt(2*pi); % normalizing coefficient for Gauss
DOS
N0n = 1.0E26; % [1/m^3] Prefactor in Gauss DOS
N0p = 1.0E26; % [1/m^3] Prefactor in Gauss DOS
Nt = 1.0E20;
sgm = 0.05; % [eV] Width of Gauss DOS for
carriers
Em = 10*sgm;
dE = sgm/10;
Ed = -Em:dE:Em; % [eV] (E-Ev), Energy variable in
Gauss DOS
GSn = N0n/CN/sgm*exp(-0.5*(Ed/sgm).^2); % Gauss DOS
GSp = N0p/CN/sgm*exp(-0.5*(Ed/sgm).^2); % Gauss DOS

al = 3.0E-10; % [m] Latice constant
af = 1/al;
mu0 = 1.0E3;

% Defining Effective Density of States %
Eg = 1.43; % [eV] Band gap

```

```

Wan      = 0.157;                                % [eV]
Wcat     = 0.15;                                 % [eV]
Vbi      = Eg-Wan-Wcat;

nan      = dE*sum(GSn./(1+exp((Ed+Eg-Wan)/Vt)));
ncat     = dE*sum(GSn./(1+exp((Ed+Wcat)/Vt)));
pan      = dE*sum(GSp./(1+exp((Wan-Ed)/Vt)));
pcat     = dE*sum(GSp./(1+exp((Eg-Wcat-Ed)/Vt)));

n1       = sqrt(nan*ncat);
p1       = sqrt(pan*pcat);
ni       = sqrt(n1*p1);
Nc       = sqrt(N0n*N0p)*exp(0.5*(sgm/Vt)^2)

gm       = 1.0;                                  % Coefficient for generation rate
Pin      = 1000;                                % [W/m^2] Incident-light power
density
% Pin      = Pind(ipin);                         % [W/m^2] Incident-light power
density
kin      = Pin/Ipt0;
Ipdb    = kin*[0.5*Ipa Ipb];
Ipfc    = Ipdb.*(wl*1.0E-9/h/cc);             % [1/m^2/s] Incident photon flux, Step
of wave-length is 0.5 nm

tn       = 1.0E-5;                             % SRH life time of electron
tp       = 1.0E-5;                             % SRH life time of hole
mun0    = 1.0E3;                              % [m^2/V-s] Electron Mobility
mup0    = 5.0E2;                              % [m^2/V-s] Hole Mobility
np0     = 1.0E50;                            % Parameter in Mobility
tx       = 2.0E-9;                            % Lifetime of exiton

% End of Definition of Material_Constants and some material constants

% Setting the size of the simulation %

xmx     = 80.0E-9;                           % [m]
nmx     = 80;
dx      = xmx/(nmx-1);
xd      = 0:dx:xmx;                          % Coordinate points

nd(1)   = nan;
nd(nmx) = ncat;
pd(1)   = pan;
pd(nmx) = pcat;

```



```

stn      = 1+0*xd;
stp      = 1+0*xd;
Cn1      = mean(mun*Ef);
Cn2      = Vt*mean(stn.*mun);
Cp1      = mean(mup*Ef);
Cp2      = Vt*mean(stp.*mup);

Vplot    = [];
Jplot    = [];
for Va = Vmn:dV:Vmх;                                % [V] Start Va increment for loop
Va
Ef       = (Va-Vbi)/xmx;                            % [V/m] Strength of electric field
Efx     = Ef+0*xd;

for js=1:10                                         % Start loop for self-consistency
tn       = eps/q/Nt./mun;
tp       = eps/q/Nt./mup;
nv       = mean(nd);
pv       = mean(pd);
mdv     = mean(nd.*pd.*(mun+mup));
kn       = q/eps*mdv/nv;
kp       = q/eps*mdv/pv;

gv       = mean(ni^2./(tp.*(nd+n1)+tn.*(pd+p1)));
npv     = mean(nd.*pd./(tp.*(nd+n1)+tn.*(pd+p1)));
gn       = npv/nv;
gp       = npv/pv;

gnv     = (1-PX)*(kn+gn);
gpv     = (1-PX)*(kp+gp);
wnt     = sqrt(Cn1^2+4*gnv*Cn2);
wpt     = sqrt(Cp1^2+4*gpv*Cp2);

dtn1    = (-Cn1-wnt)/2/Cn2;
dtn2    = (-Cn1+wnt)/2/Cn2;
dtp1    = (-Cp1-wpt)/2/Cp2;
dtp2    = (-Cp1+wpt)/2/Cp2;

Bn1     = -gm./(Cn2*cas.^2-Cn1*cas-gnv);
Bn2     = -gm./(Cn2*cas.^2+Cn1*cas-gnv);
Bp1     = -gm./(Cp2*cas.^2+Cp1*cas-gpv);
Bp2     = -gm./(Cp2*cas.^2-Cp1*cas-gpv);

% Calculate gn, gn1, gp, gp1

```

```

for i=1:nmx
    gn(i) = gv/gnv+PX*sum((Bn1.*exp(-cas*xd(i))+Bn2.*exp(-cas*(2*xmx-
xd(i))).*Ipf.*cas);
    gn1(i) = PX*sum((-Bn1.*exp(-cas*xd(i))+Bn2.*exp(-cas*(2*xmx-
xd(i))).*Ipf.*cas.^2);
    gp(i) = gv/gpv+PX*sum((Bp1.*exp(-cas*xd(i))+Bp2.*exp(-cas*(2*xmx-
xd(i))).*Ipf.*cas);
    gp1(i) = PX*sum((-Bp1.*exp(-cas*xd(i))+Bp2.*exp(-cas*(2*xmx-
xd(i))).*Ipf.*cas.^2);
end

An1 = ((nd(1)-gn(1))*exp(dtn2*xmx)-nd(nmx)+gn(nmx))/(exp(dtn2*xmx)-
exp(dtn1*xmx));
An2 = ((nd(1)-gn(1))*exp(dtn1*xmx)-nd(nmx)+gn(nmx))/(exp(dtn1*xmx)-
exp(dtn2*xmx));
Ap1 = ((pd(nmx)-gp(nmx))*exp(dtp2*xmx)-pd(1)+gp(1))/(exp(dtp2*xmx)-
exp(dtp1*xmx));
Ap2 = ((pd(nmx)-gp(nmx))*exp(dtp1*xmx)-pd(1)+gp(1))/(exp(dtp1*xmx)-
exp(dtp2*xmx));

% Calculate nd, nd1, pd, pd1
nd = An1*exp(dtn1*xd)+An2*exp(dtn2*xd)+gn;
nd1 = An1*dtn1*exp(dtn1*xd)+An2*dtn2*exp(dtn2*xd)+gn1; %
derivative of nd to x
pd = Ap1*exp(dtp1*(xmx-xd))+Ap2*exp(dtp2*(xmx-xd))+gp;
pd1 = -Ap1*dtp1*exp(dtp1*(xmx-xd))-Ap2*dtp2*exp(dtp2*(xmx-xd))+gp1; %
derivative of pd to x

% Calculate Jn, Jnv, Jp, Jpv
Jnv = q*nd*Cn1+q*Cn2*nd1;
Jpv = q*pd*Cp1-q*Cp2*pd1;
Jtv = mean(Jnv+Jpv);

% yn = 0*xd;
% yp = 0*xd;
for j=1:5
    for i=1:nmx
        yn(i) = nd(i)/(dE*sum(GSn./(yn(i)+exp(Ed/Vt))));
        yp(i) = pd(i)/(dE*sum(GSp./(yp(i)+exp(-Ed/Vt))));
    end
end
for i=1:nmx
    stn(i) =
sum(GSn./(yn(i)+exp(Ed/Vt)))/sum(GSn.*exp(Ed/Vt)./(yn(i)+exp(Ed/Vt)).^2);

```

```

    stp(i) = sum(GSp./(yp(i)+exp(-Ed/Vt)))/sum(GSp.*exp(-Ed/Vt)./(yp(i)+exp(-
    Ed/Vt)).^2);
    end

    for i=1:nmx
        mun(i) = MoPSV(N0n,sgm,mun0,al,T,Efx(i),nd(i));
        mup(i) = MoPSV(N0p,sgm,mup0,al,T,Efx(i),pd(i));
        end

        Jn = q*Efx.*nd.*mun+kb*T*stn.*mun.*nd1;
        Jp = q*Efx.*pd.*mup-kb*T*stp.*mup.*pd1;
        Jt = mean(Jn+Jp); % total

photocurrent

    Edx = 0*xd;
    for i=2:nmx
        Edx(i) = Edx(i-1)+q/eps*dx*pd(i-1);
    end
    Efl = (Va-Vbi)/xmx-dx/xmx*sum(Edx);
    Efx = Efl+Edx;

    Cn1 = mean(mun.*Efx.*nd)/mean(nd);
    Cn2 = Vt*mean(stn.*mun.*nd1)/mean(nd1);
    Cp1 = mean(mup.*Efx.*pd)/mean(pd);
    Cp2 = Vt*mean(stp.*mup.*pd1)/mean(pd1);

%     erj = 100*abs(Jt./Jtv-1)
% end % end of loop for js in line 158

erj = 100*abs(Jt./Jtv-1)
Vplot = [Vplot,Va];
Jplot = [Jplot,Jt];

%
figure(3)
plot(xd, mun,'--b',xd,mup,'--b','LineWidth',2); hold on;
%
figure(4)
plot(xd, stn,'--b',xd,stp,'--b','LineWidth',2); hold on;
%
figure(5)
plot(xd, Jtv,'or',xd,Jt,'+b','LineWidth',2); hold on;
%
figure(6)
plot(xd, nd,'-r',xd,pd,'--b','LineWidth',2); hold on;
%
figure(6)
plot(xd, Efx,'-r','LineWidth',2); hold on;

```

```

%%%%%%%%%%%%%%%
%%%%% END OF NON-EQUILIBRIUM SOLUTION PART
%%%%%
%%%%%%%%%%%%%%%
%%%%% Loop for Va
end

figure(9)
plot(Vplot, Jplot,'-r','LineWidth',2); hold on;
axis([0 1.2 -300 10]);
xlabel('V [V]');
ylabel('J [A/m^2]');
title('J vs V');

% Following data read from [Fine-tuning of side-chain orientations on nonfullerene acceptors
enables
% organic solar cells with 17.7% efficiency, Gaoda Chai et al. Energy Environ. Sci. 14, 3469
(2021)]
% Vfig=[431 493 557 621 685 748 811 875 940 1004 1067 1131 1195 1258 1322 1386
1450 1515 1554 1578 1608]; % PTQ10:o-BTP-PhC6
% Jfig=[987 985 985 985 982 980 980 978 975 972 969 964 962 954 944 923 879 754 580
414 131]; % PTQ10:o-BTP-PhC6
%
% Vfig=[431 493 557 621 685 748 811 875 940 1004 1067 1131 1195 1258 1322 1386 1450
1491 1515 1538 1554]; % PTQ10:m-BTP-PhC6
Jfig=[1082 1082 1080 1079 1078 1077 1076 1074 1070 1068 1066 1061 1060 1050 1038
1007 915 756 598 339 131]; % PTQ10:m-BTP-PhC6
%
% Vfig=[431 493 557 621 685 748 811 875 940 1004 1067 1131 1195 1258 1322 1386
1450 1492 1515 1544 1561]; % PTQ10:p-BTP-PhC6
% Jfig=[1057 1056 1055 1055 1053 1052 1049 1047 1045 1043 1038 1037 1030 1023 1011
984 904 768 636 351 131]; % PTQ10:p-BTP-PhC6

Vexp=0+0.8*(Vfig-431)/(1450-431); %
Unit [V]
Jexp=10*(-25+25*(Jfig-1070)/(132-1070)); % Unit
from [mA/cm^2] to [A/m^2]
% Above data read from [Fine-tuning of side-chain orientations on nonfullerene acceptors
enables
% organic solar cells with 17.7% efficiency, Gaoda Chai et al. Energy Environ. Sci. 14, 3469
(2021)]

```



